Interpretation of residual gravity anomalies caused by simple geometrical shapes using the improved Grey Wolf Optimisation algorithm

M. Ahmadi¹, A. Akbari Dehkharghani¹ and A.N. Kalateh²

- ¹ Department of Petroleum, Mining and Materials Engineering, CT.C., Islamic Azad University, Tehran, Iran
- ² Department of Mining, Petroleum, and Geophysics, Shahrood University of Technology, Shahrood, Iran

(Received: 22 September 2023; accepted: 29 July 2025; published online: 28 November 2025)

ABSTRACT

In this research, an algorithm inspired by nature, i.e. the Improved Grey Wolf Optimiser (IGWO), is used in an iterative process to simultaneously estimate the optimal value of parameters related to simple geometric models (sphere, horizontal cylinder, and vertical cylinder) in a multi-objective problem. The variables of each model are the parameters of the amplitude coefficient (A), depth (z), shape factor (q), and position of the model centre (x). In this modelling, each of the wolves are a model having the dimensions of the numbers of the model parameters. This algorithm was verified in two stages. First, the accuracy of the algorithm was investigated for the gravity data generated from the artificial models of the sphere, horizontal cylinder, vertical cylinder, and a combination of different models in two states, i.e. with and without noise. The results show that the values of the parameters obtained with the IGWO are almost equal to the actual parameters. Also, by adding noise to the data, the results are satisfactory. In the next step, the real gravity data related to two abnormality profiles from Iran and America were used in this modelling. In this step, the comparison between the results of the IGWO algorithm and the results of previous studies indicated the proper performance of the proposed method. The inversion results obtained with the mentioned method show that the amplitude coefficient, depth, and shape factor of the salt dome located in America are respectively about -270.32 mGal×km², 4.54 km, and 1.51, and of the salt dome located in Iran are -270.32 mGal×km², 63.83 m, and 1.49. The advantage of IGWO inversion is that it has few parameters to adjust, it estimates the optimal value of the parameters quickly, and also converges with a nonlinear convergence coefficient without getting stuck in local minima.

Key words: gravity anomaly, inverse modelling, optimisation, IGWO algorithm, salt dome.

1. Introduction

Inverse problems in gravimetry mainly seek to acquire information on the structure inside the Earth through measurements performed on its surface. However, the main issue in solving such problems is given by the non-uniqueness of the answer of the same (Barbosa and Silva, 1994).

Due to limitations and weaknesses in measurements and analytical methods, there may be multiple acceptable models and hypotheses for a set of data, leading to different descriptions

© 2025 - The Author(s)

of the Earth's structure. In other words, it is not possible to provide a unique and definite model for the geological structure with absolute accuracy. For this reason, in such problems, the effort is directed towards finding the best-fitting model that aligns with the available data and optimally estimates the geological structure. This process may involve complex analytical and computational methods, accompanied by various assumptions and estimations.

Inverse problems are classified into the two categories of linear and nonlinear inverse problems. Nonlinear inverse problems include a nonlinear relationship between model parameters and observed values. Modelling geometrical parameters, such as depth and thickness, are mainly nonlinear. Interpretation of geophysical data, such as gravimetry data, seeks to obtain the geometrical parameters of gravity anomalies. This interpretation, which in fact consists in solving an inverse problem, is built on the basis of simple geometrical shapes (e.g. cylinders and spheres) due to their structural similarity to materials examined in exploratory studies. Simulating the structure of mineral masses, that generate gravity anomalies in a geometrical shape, requires field and geological survey. For these gravity models, simple formulae have been proposed to calculate gravity anomaly with a good approximation. These formulae are adjusted based on the shape and characteristics of mineral deposits and subsurface structures. They assist us in obtaining a more accurate estimation of areas with gravity anomalies.

In nonlinear inverse modelling problems, there is a direct connection with random sampling methods and Bayesian frameworks. Bayesian methods have wide applications in the field of geophysical inverse modelling. This stems from the fact that geophysical surveys are essentially conducted within the framework of prior information and assumptions, with the aim of updating and refining existing knowledge. Bayesian methods enable the combination of prior probabilistic information with data obtained from surveys, enabling for the updating and enhancement of the overall information set (Bosch, 1999; Calcagno *et al.*, 2008; Rossi *et al.*, 2015).

Nonlinear inversion techniques can practically be divided into the two groups of local search techniques based on the information of target function gradient changes (steepest descent method, conjugate gradient, Levenberg–Marquardt method) and general search techniques (simulated annealing, genetic algorithms, particle swarm optimisation, ant colony) based on physical processes and phenomena present in nature (Snieder, 1998; Tarantola, 2005; Yuan *et al.*, 2009). An initial assumption, used in the local search techniques, is the same as the geometrical shape of some anomaly sources. The accuracy of the results depends on how close, in terms of shape, the assumed model is to the real structure.

Among these techniques, the least-square minimisation (Gupta, 1983; Abdelrahman *et al.*, 1991; Salem *et al.*, 2003), Mellin transformation (Mohan *et al.*, 1986; Babu *et al.*, 1991), Fourier transformation (Odegard and Berg, 1965; Sharma and Geldart, 1968), Euler deconvolution (Thompson, 1982; Reid, 1990), and Werner deconvolution (Hartman *et al.*, 1971; Kilty, 1983) techniques are worthy of mention. Moreover, techniques such as the analytical signal (Nandi *et al.*, 1997), Walsh transformation (Shaw and Agarwal, 1990), and nonlinear least square minimisation (Abdelrahman and El-Araby, 1993; Abdelrahman and Sharafeldin, 1995a, 1995b; Abdelrahman *et al.*, 2001; Essa, 2014) have also been proposed to estimate the factor of gravity anomaly source.

Additionally, several computational methods for gravity data inversion have been proposed to estimate model parameters with varying levels of success (Li and Chouteau, 1998; Li and Oldenburg, 1998; Boulanger and Chouteau, 2001). A simple method, suggested by Essa (2007), uses the residual gravity anomalies along a profile to determine the depth and shape factor of simple geometric bodies. Another automated method is the least-square method, proposed by Asfahani and Tlas (2008). This method calculates the depth and amplitude coefficient. In

addition to these methods, Asfahani and Tlas (2012) developed the fair function minimisation procedure. Fedi (2007) proposed a method called depth from extreme points to interpret any potential field. Furthermore, the regularised inversion method was developed by Mehanee (2014).

General search techniques, such as neural networks and metaheuristic algorithms, have recently been used to obtain the general optimised answer or exit from the local optimal answer when solving geophysical inverse problems, e.g. to estimate the parameters of simple geometrical shapes. Some of these techniques include the teaching-learning-based optimisation algorithm, gravity and magnetic data interpretation (Eshaghzadeh and Hajian, 2020; Eshaghzadeh and Sahebari, 2020), the tuned particle swarm algorithm (Roshan and Singh, 2017), simulated annealing algorithm (Biswas, 2015), particle swarm algorithm (Essa and Elhussein, 2018), and whale algorithm (Vashisth *et al.*, 2019). One of the most important features of metaheuristic algorithms is that they do not fall into the local minimum trap and have been claimed, by previous studies, to be more accurate than other algorithms.

The Grey Wolf Optimiser (GWO) is a nature-inspired metaheuristic optimisation method used in various problems. The GWO algorithm is a swarm intelligence algorithm and has fewer parameters to adjust. Other sciences have proposed various types of GWO algorithm in recent years. Sulaiman *et al.* (2015) demonstrated the effectiveness of the GWO in reactive power dispatch problems. Kamboj (2016) used this algorithm to solve the economic dispatch problem. Song *et al.* (2015) used this algorithm for an inverse problem in surface waves and Agarwal *et al.* (2018) used it to optimise geophysical data in a thin dike.

Improved algorithms based on the GWO are also used to foster greater balance between exploitation and exploration seeking to prevent getting trapped in local optima and to increase the convergence speed (Muangkote *et al.*, 2014; Al-Attar *et al.*, 2015; Zhu *et al.*, 2015; Mittal *et al.*, 2016; Chahar and Kumar, 2017; Heidari and Pahlavani, 2017; Jadhav and Gomathi, 2017).

The present study has used the Improved GWO (IGWO) to calculate the amplitude coefficient (A), depth (z), shape factor (q), and model centre position (x_0) of the gravity anomaly source. The algorithm was validated using the vertical-cylinder, horizontal-cylinder, and sphere synthetic models as well as the compound model with and without noise. Moreover, two gravity anomaly profiles from Iran and the U.S.A. were used for inversion. In this study, modelling codes have been prepared with MATLAB software.

2. Theoretical basis

2.1. Forward modelling for synthetic data production

Gravity anomaly for sphere, infinitely long horizontal-cylinder, and semi-infinite vertical-cylinder structures (Fig. 1) have been proposed as follows (Abdelrahman *et al.*, 1989):

$$G(xi, z, q) = A \frac{z^m}{(x_i^2 + z^2)^q}$$
 (1)

where m=1 and $A=\frac{4}{3}\pi G\sigma R^3$ for the sphere, m=1 and $A=2\pi G\sigma R^2$ for the horizontal cylinder, and m=0 and $A=2\pi G\sigma R^2$ (R<<Z) for the vertical cylinder. The geometric shape factor (q) was 1.5, 1, and 0.5 for the sphere, horizontal and vertical cylinders, respectively. A is the amplitude

coefficient, z indicates depth, G represents universal gravity, σ is density contrast, R is radius, and x_i is the horizontal position coordinate of the buried structure.

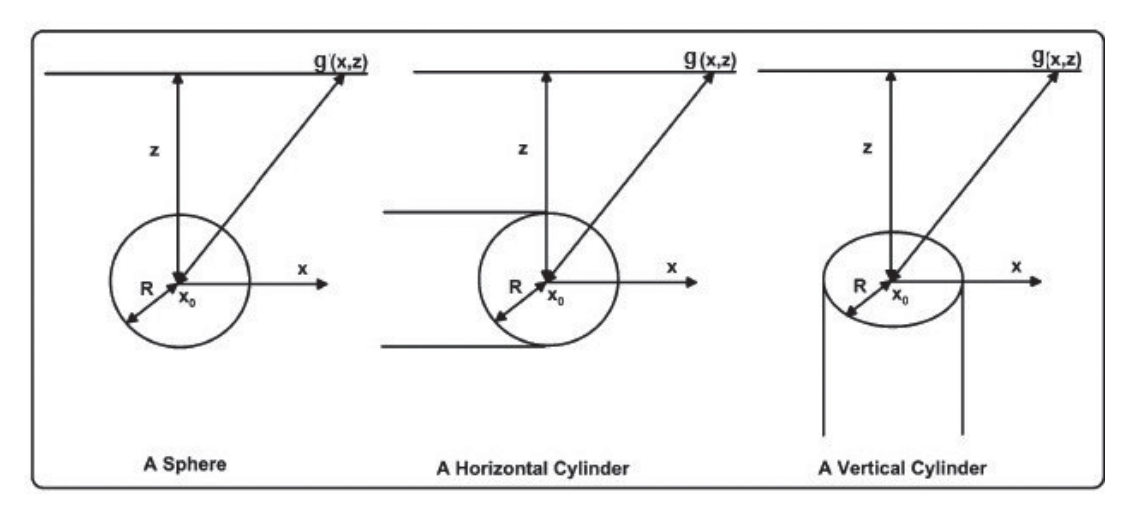


Fig. 1 - Demonstration of the simple geometric structures (sphere and cylinders).

2.2. Grey Wolf Optimiser (GWO)

Proposed by Mirjalili *et al.* (2014), the GWO is a population-based metaheuristic algorithm inspired by the social behaviour of grey wolves in nature and their manner of hunting (Mirjalili *et al.*, 2014).

The wolves are classified into the four groups of α , β , δ , and ω based on the social hierarchy. The α wolves are assumed to be the main drivers of the algorithm, while the β and δ wolves perform as the assistants of the alphas and the rest (omegas) are considered their followers. Collective hunting is among the wolves' behaviours and comprises tracking on, surrounding, and attacking the prey.

2.2.1. Mathematical modelling of the GWO algorithm

Each grey wolf is first considered as a search agent and evaluated based on the value of the cost function which considers the best position (solution), such as α , β , and δ that are assumed to better inform of the potential prey's location, while the other solutions are entitled omegas. Each ω wolf updates its position based on the position of the best search agents (α , β , and δ). Eqs. (2) to (7) are used to model the aforementioned:

$$\vec{D}_{\alpha}(t) = \left| \overrightarrow{C}_{1} * \vec{X}_{\alpha}(t) - \vec{X}(t) \right|,$$

$$\vec{D}_{\beta}(t) = \left| \overrightarrow{C}_{2} * \vec{X}_{\beta}(t) - \vec{X}(t) \right|,$$

$$\vec{D}_{\delta}(t) = \left| \overrightarrow{C}_{3} * \vec{X}_{\delta}(t) - \vec{X}(t) \right|$$
(2)

$$\vec{X}_{1}(t) = \vec{X}_{\alpha}(t) - A_{1} * \vec{D}_{\alpha}(t),
\vec{X}_{2}(t) = \vec{X}_{\beta}(t) - A_{2} * \vec{D}_{\beta}(t),
\vec{X}_{3}(t) = \vec{X}_{\delta}(t) - A_{3} * \vec{D}_{\delta}(t)$$
(3)

where $\vec{X}(t)$ is the position of grey wolf ω in the t^{th} iteration (current state), and $\vec{X}_{\alpha}(t)$, $\vec{X}_{\beta}(t)$, and $\vec{X}_{\delta}(t)$ are the position vectors of α , β , and δ in the t^{th} iteration [Eqs. (2) and (3) are valid for a generic ω wolf].

Moreover,

$$\vec{A} = \vec{a}(2\vec{r}_1 - 1) \tag{4}$$

$$\vec{C} = 2\vec{r}_2 \tag{5}$$

$$a = 2 - 2 * t/t_{max} \tag{6}$$

where \overrightarrow{A} and \overrightarrow{C} are the coefficient vectors obtained from Eqs. (4) and (5), with r_1 and r_2 random vectors between [0, 1], and a, obtained from Eq. (6), where t represents the number of current iteration and t_{\max} represents the maximum number of iterations, reduces linearly from two to zero given the number of iterations.

The new position of each point is ultimately obtained from all three solutions and

$$\vec{X}(t+1) = \frac{\vec{X}_1(t) + \vec{X}_2(t) + \vec{X}_3(t)}{3} \tag{7}$$

where $\vec{X}(t+1)$ is the location variable in the next state. The next iteration takes place afterwards, which means that the new α , β , and δ are selected among all the population and the same process is repeated. After the final iteration, α is identified as the optimal point.

2.2.2. Exploration and exploitation

In the preying stage, the wolves separate from one another to explore the various points of the solution environment. The random vector \overrightarrow{A} with a value of A > 1 is used to mathematically model this process, and when A < 1, the wolves are converged towards the prey which helps establish a balance between exploration and exploitation. In this algorithm, half of the iterations are concerned with exploration and the other half are concerned with exploitation.

2.3. Improved Grey Wolf Optimiser (IGWO)

Considering the characteristics of geophysical inverse problems, the original GWO algorithm has been enhanced to ensure its effectiveness in geophysical inversion tasks. Firstly, an improved convergence factor has been introduced to better handle the nonlinear inverse problem. Secondly, the equations of the traditional location updating strategy, based on the differences in the fitness values of α , β , and δ , have been modified. This enhanced version of the GWO algorithm is referred to as IGWO.

Convergence factor a in the GWO algorithm varies linearly from 2 to 0. In this paper, for a better balance between exploration and exploitation, the equation for the convergence factor has been modified as follows:

$$a = 2\left[1 - \left(\frac{t-1}{t_{max}-1}\right)^{1.5}\right]. \tag{8}$$

In Eq. (8), the convergence factor a is described as an exponential change. In the original GWO algorithm, half of the iterations are allocated for exploration and the other half for exploitation. By using the modified convergence factor, a greater number of iterations are dedicated to exploration, which helps prevent local minima. With this type of nonlinear convergence factor, the percentages of iterations used for exploration and exploitation are approximately 60% and 40%, respectively (Li *et al.*, 2018).

In the GWO algorithm, the new position of each wolf is determined on the basis of the positions of the three wolves: α , β , and δ . Eq. (3) represents the new positions of wolf α $[\vec{X}_1(t)]$, wolf β $[\vec{X}_2(t)]$, and wolf δ $[\vec{X}_3(t)]$. Other search agents (ω) update their positions based on the positions of the best search agents [Eq. (7)].

The drawback of this equation is that it treats the positions of the three main wolves, α , β , and δ , equally, as the new position of the ω wolf is derived from the average of these three wolves. This approach disregards the social hierarchy within the wolf pack. In the improved algorithm, the new position of the ω wolf is determined based on the superiority percentage of the three wolves according to the hierarchical pyramid. The new position of the ω wolf is calculated with a weight that corresponds to the hierarchy, giving a higher percentage to the α wolf and a lower percentage to the other two wolves:

$$x = x_{\alpha} \cdot \left[\frac{Q(\alpha)}{Q(\alpha) + Q(\beta) + Q(\delta)} \right] + x_{\beta} \cdot \left[\frac{Q(\beta)}{Q(\alpha) + Q(\beta) + Q(\delta)} \right] + x_{\delta} \cdot \left[\frac{Q(\delta)}{Q(\alpha) + Q(\beta) + Q(\delta)} \right]. \tag{9}$$

In Eq. (9), $Q_{(\alpha)}$, $Q_{(\beta)}$, and $Q_{(\delta)}$ represent the cost function value for α , β , and δ in the t^{th} iteration, respectively. Fig. 2 shows the flowchart of the IGWO algorithm.

3. IGWO algorithm implementation on gravity data

In this study, the feasibility of applying the IGWO algorithm in modelling nonlinear shapes of simple geometric forms using gravity data will be investigated. In the mentioned modelling, the unknowns of the problem are the parameters of amplitude coefficient (A), depth (z), shape factor (q), and the centre position of the body (x_0). In other words, each model (wolf) represents the assumed parameters. In the IGWO algorithm, each grey wolf serves as a representative solution; thus, in this study, each grey wolf is essentially an n-dimensional vector representing n unknown parameters. For each grey wolf, the value of the objective function can be calculated as follows (Santos, 2010):

$$C = \frac{2 \sum_{i}^{N} |g_{i}^{o} - g_{i}^{c}|}{\sum_{i}^{N} |g_{i}^{o} - g_{i}^{c}| + \sum_{i}^{N} |g_{i}^{o} + g_{i}^{c}|}$$
(10)

where g_i^o is the observed gravity, g_i^c is the calculated gravity, and N is the number of gravity measurement points.

For this purpose, the two-dimensional gravity fields for these geometric shapes have been calculated. The obtained gravity fields, in the form of a gravity vector, are provided as input to the software. Inversion is performed using noise-free synthetic data and by adding 10% noise to recover the true parameters of the model. Initially, the ranges for the unknown parameters (A, z, q, x_0) are introduced to the IGWO, and should include the assumed values for the initial model.

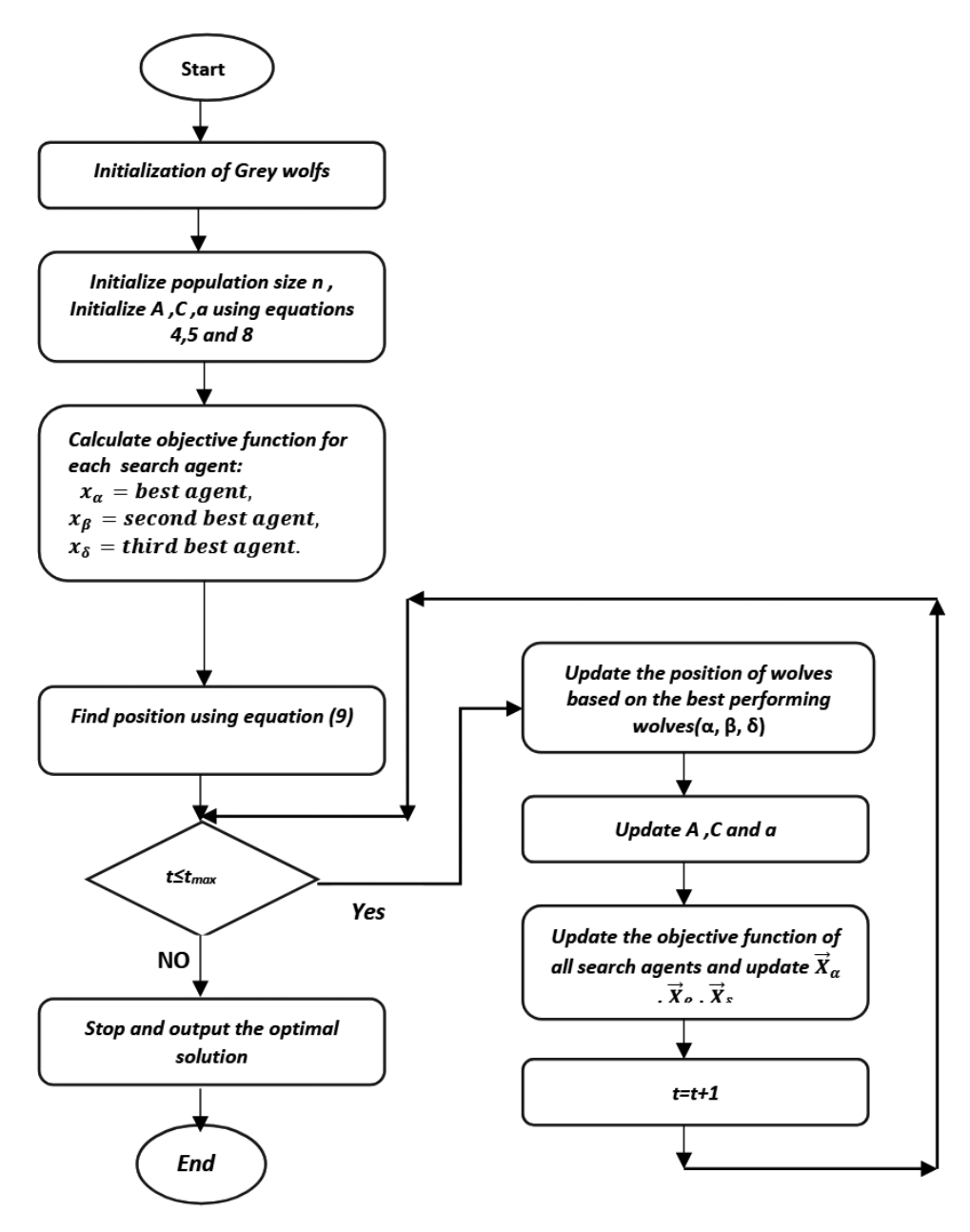


Fig. 2 - The flowchart of the IGWO algorithm.

For modelling with the IGWO algorithm, 50 initial models are generated based on the specified range for parameters such as domain coefficient, depth, shape factor, and the centre position of the model.

In each iteration, the parameter values change and the gravity field for the new variables is calculated. The error between the calculated and observed gravity fields is determined. The minimum error, based on the objective function (equation), is set to 0.01 for stopping the iterations. The desired number of iterations for each program run is 300, during which the final values for each parameter are stored.

4. Method validation through synthetic models

4.1. Single-source models

The three sphere, vertical-cylinder, and horizontal-cylinder models were considered along a profile as long as 200 km with sampling distances of 1 km [so that the axes of all three models were placed in the origin ($x_0 = 0$)] to evaluate the efficiency of the proposed method. The assumed variables in the aforementioned models were z = 20 km, A = 300 mGal×km², and q = 1.5 for the sphere; z = 20 km, A = 300 mGal×km, and q = 1 for the horizontal cylinder; and z = 20 km, z = 20 km

Random 10 % noises were added to the data as per Eq. (11) to simulate natural conditions, where $g_{obs}(x_i)$ is the noise corrupted synthetic data at x_i and RND(i) is a pseudorandom number whose range is between 0 and 1:

$$g_{noise} = g_{obs}(x_i) [1 + (RND(i) - 0.5) \times 0.1].$$
 (11)

Figs. 3 to 5 illustrate the observed and calculated anomalies with and without 10% noise for all three models mentioned above. The present study used the statistical criterion of root-mean-square error (*RMSE*) which indicates the difference between the observed gravity and the gravity calculated based on the estimation parameters so as to analyse the quality of the IGWO results. Tables 1 to 3 demonstrate the *RMSE* results for the sphere, horizontal-cylinder, and vertical-cylinder models, respectively.

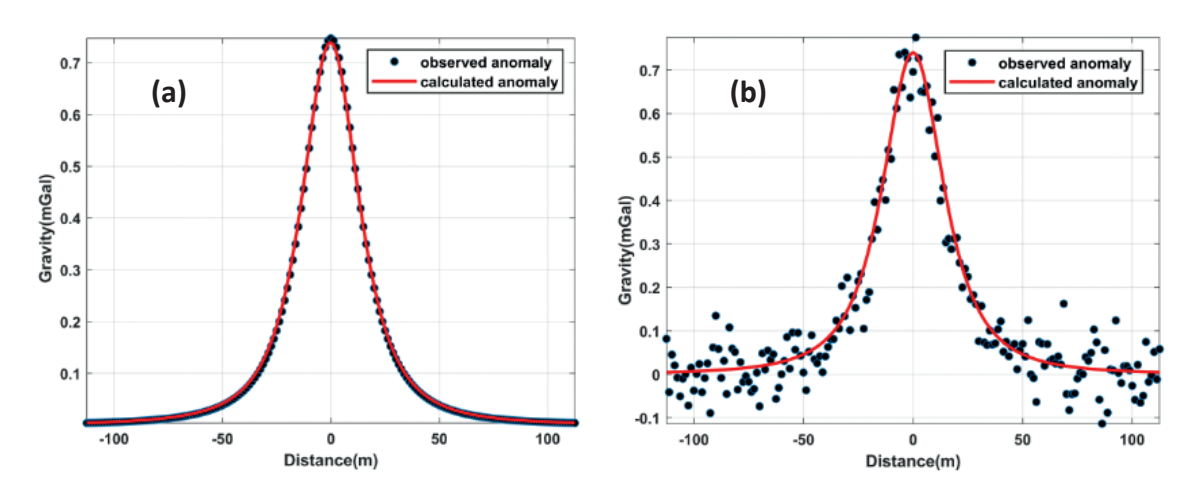


Fig. 3 - The effect of observed gravity anomaly and gravity anomaly produced by IGWO inversion for the sphere model with a) no noise and b) 10% noise.

Table 1 - The parameters estimated by the IGWO for the sphere model.

Parameter	Initial value	Search range	Without noise	With noise (10%)
A (mGal×km²)	300	250 to 350	316.41	250.59
z (km)	20	10 to 30	20.14	20.80
q	1.5	0 to 2.5	1.5	1.45
x ₀ (km)	0	-5 to 5	0.0042	-0.22
RMSE (mGal)			0.00003	0.0494

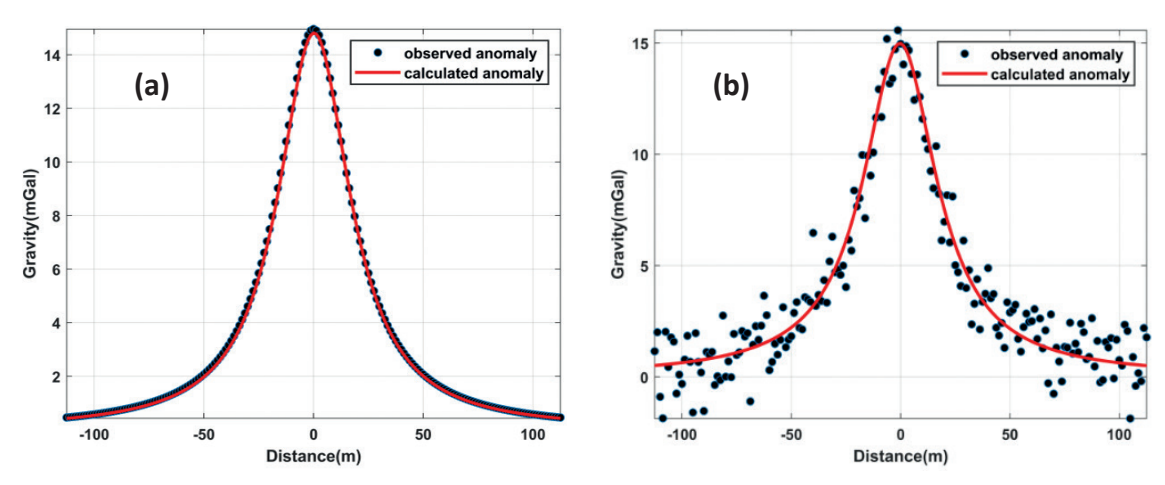


Fig. 4 - The effect of observed gravity anomaly and gravity anomaly produced by IGWO inversion for the horizontal-cylinder model with a) no noise and b) 10% noise.

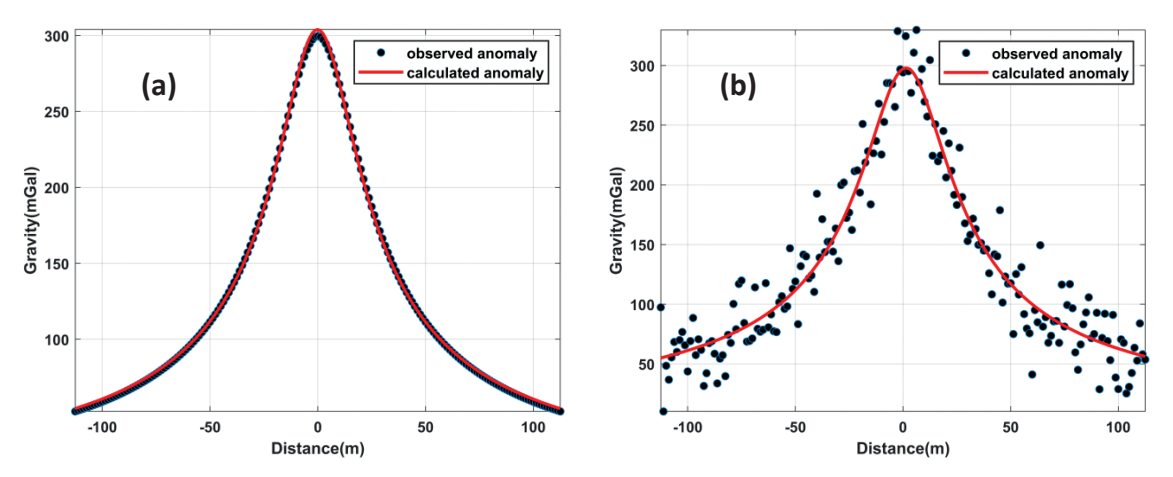


Fig. 5 - The effect of observed gravity anomaly and gravity anomaly produced by IGWO inversion for the vertical-cylinder model with a) no noise and b) 10% noise.

Table 2 - The parameters estimated by the IGWO for the horizontal-cylinder model.

Parameter	Initial value	Search range	Without noise	With noise (10%)
A (mGal×km)	300	250 to 350	306.49	250.02
z (km)	20	10 to 30	20.08	20.12
q	1	0 to 2	1.003	0.97
<i>x</i> ₀ (km)	0	-5 to 5	0463	-0.571
RMSE (mGal)			0.0099	1.034

In this study, the *RMSE* statistical criterion is used to compare the measured gravity field and the calculated gravity field obtained by the estimated parameters. The *RMSE* is obtained from Eq. (12), where $g(x_i)$ represents the observed gravity values and $g(x_i)$ the calculated gravity values:

Parameter	Initial value	Search range	Without noise	With noise (10%)
A (mGal×km)	300	250 to 350	301.49	257.30
z (km)	20	10 to 30	20.07	19.54
q	0.5	0 to 2	0.50	0.47
x ₀ (km)	0	-5 to 5	0.0093	1.246
RMSE (mGal)			0.0616	6.994

Table 3 - The parameters estimated by the IGWO for the vertical-cylinder model.

$$RMSE = \sqrt{\frac{\sum_{i=1}^{N} [g(x_i) - g_c(x_i)]^2}{N}}.$$
 (12)

The error values between the gravity field values of the synthetic models and the gravity field values calculated from the optimised parameters obtained with the GWO algorithm (Figs. 3 to 5) are provided in Tables 1 to 3. The smaller the calculated error, the more it confirms the optimised parameters of shape factor, amplitude coefficient, and depth for the gravity anomaly, based on which the calculated gravity field is estimated.

Regarding the search range, metaheuristic algorithms have the ability to return the actual value with some error within any search range. For example, for the horizontal-cylinder model (with a larger search range), the obtained values do not differ significantly from the search range mentioned in this study. The search range considered in this study is based on previous similar studies.

Parameter	Initial value	Search range	Without noise	With noise (10%)
A (mGal×km)	300	-200 to 1000	315.02	282.87
z (km)	20	0 to 100	20.035	19.70
q	1	0 to 5	1.008	0.95
<i>x</i> _o (km)	0	-50 to 50	0.33	0.023

Table 4 - The parameters estimated by the IGWO for the horizontal-cylinder model (with a larger search range).

4.2. Composite model (three-source)

To perform a closer evaluation of the validity of the ICWO method, Fig. 6 indicates the gravity anomaly of a composite model encompassing all three sphere and horizontal- and vertical-cylinder models along a 100-kilometre profile with data sampling distances of 1 km. In this composite model, the vertical-cylinder model was considered the target anomaly source to examine and estimate parameters with an amplitude coefficient of 400 mGal×km at 5- and 40-kilometre depths of the origin, while the horizontal cylinder (z = 10 km, $A = 800 \text{ mGal} \times \text{km}$, situated 65 km of the origin) and sphere (z = 9 km, $A = 3000 \text{ mGal} \times \text{km}^2$, situated 15 km of the origin) models were considered as false anomalies adjacent to the target anomaly. The following equation calculated the total gravity field:

$$\Delta g(x_i) = g(x_i)_{sphere} + g(x_i)_{horizontal\ cylinder} + g(x_i)_{vertical\ cylinder}. \tag{13}$$

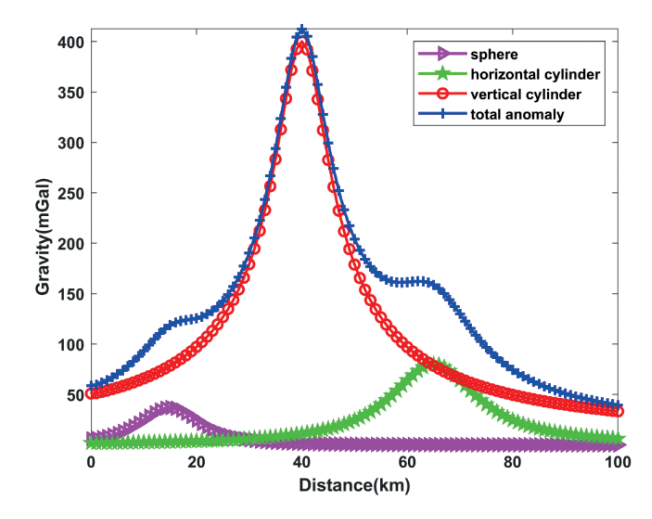


Fig. 6 - Total gravity anomaly generated by a verticalcylinder model (target anomaly) and the sphere and horizontal-cylinder models (interference agent anomalies).

The proposed algorithms were implemented for a total anomaly without noise and with 7% noise (Figs. 7a and 8a). The IGWO algorithm was implemented on the target function with 30 iterations and the obtained parameters were averaged. Table 5 reports the search range and estimated numerical results for the parameters of the vertical-cylinder model using IGWO inversion. Moreover, Figs. 7b and 8b show the convergence diagrams associated with the target function.

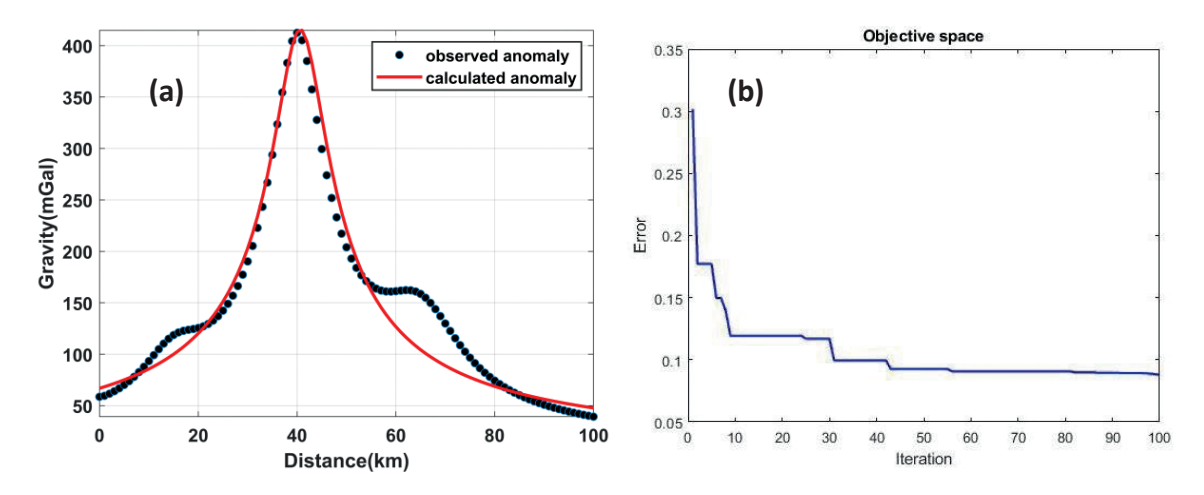


Fig. 7 - The effect of total gravity anomaly observed (combination of sphere and vertical and horizontal cylinders) and calculated through IGWO inversion (red curve) without noise (a) and the convergence diagrams associated with the target function based on the number of iterations to obtain the best response using the IGWO (b).

5. Real data modelling

In this section, two real sets of gravity data from previously-studied salt domes were inverted through the IGWO, and the calculated parameters were compared to the results obtained from other methods in previous research. A search range was first determined for each

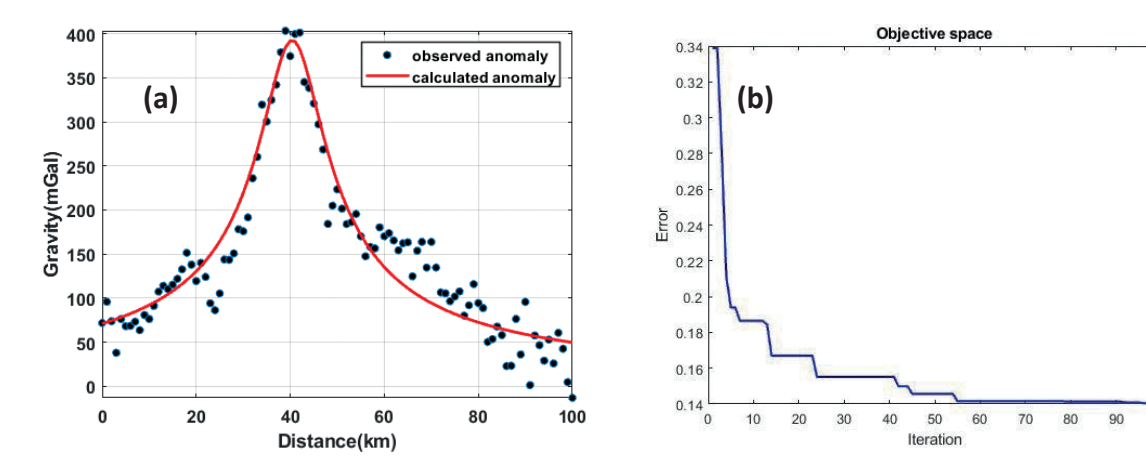


Fig. 8 - The effect of total gravity anomaly observed with noise 7% (combination of sphere and vertical and horizontal cylinders) and calculated through IGWO inversion (red curve) without noise (a) and the convergence diagrams associated with the target function based on the number of iterations to obtain the best response using the IGWO (b).

Table 5 - Initial values and estimated numerical results for target anomaly parameters (vertical-cylinder model) using the IGWO without noise and with 7% noise.

Parameter	Initial value	Search range	Without noise	With noise (7%)
A (mGal×km)	400	350 to 450	380.01	350.03
z (km)	5	2 to 8	5.06	5.2
q	0.5	0 to 2	0.48	0.46
<i>x</i> ₀ (km)	40	20 to 60	40.33	40.67
Cost function (q)			0.096	0.145

model parameter. The depth range, amplitude coefficient, and shape factor parameters must be determined based on the real gravity field data, geological information of the region, and anomaly shape for real gravity data. The first 100 initial models were randomly considered for all gravity anomaly data. The salt domes presented negative gravity contrasts due to their lower density compared to the surrounding sites and, thus, appeared as negative anomalies on gravity maps.

5.1. The Humble salt dome

The Humble oil field salt dome is situated 2 km from Humble town, on the north coast of the Texas Gulf Coast in Kansas, U.S.A. (Fig. 9). The studied reservoir rock was a limestone and anhydrite formation from the Miocene, Oligocene, Eocene, and Pliocene periods. Oil traps were observed in both cap rock and slopes of the Humble salt dome.

One profile (AA') was prepared in the NE-SW direction with a length of 4.8 km using Geosoft software whose numerical values were used as the input of the program. Datum collection was carried out on the AA' profile in 24 points at 0.2-kilometre intervals. Fig. 11 illustrates the anomaly generated by this profile and the results of inverse modelling using the IGWO.

Table 6 shows the values obtained for the residual gravity anomaly with the method discussed above, where the depth to the centre of the model is 4.5 km and a geometric shape factor of

1.52 was obtained. The sphere model was, thus, revealed to be the best model to simulate this anomaly. Several approaches have been employed by different researchers to determine the parameters of the Humble salt dome, as summarised in Table 6. These include the three least-squares minimisation technique (Abdelrahman *et al.*, 2001), the simple formula method (Salem *et al.*, 2003), a versatile nonlinear inversion approach (Tlas *et al.*, 2005), the regularised inversion method (Mehanee, 2014), very fast simulated annealing global optimisation (Biswas, 2015), and the fair function minimisation technique (Asfahani and Tlas, 2012). The depth estimated in the present study using the IGWO method is 4.5 km, which shows good agreement with previously reported values of 5.58 km by Asfahani and Tlas (2012) and 5.59 km by Tlas *et al.* (2005).

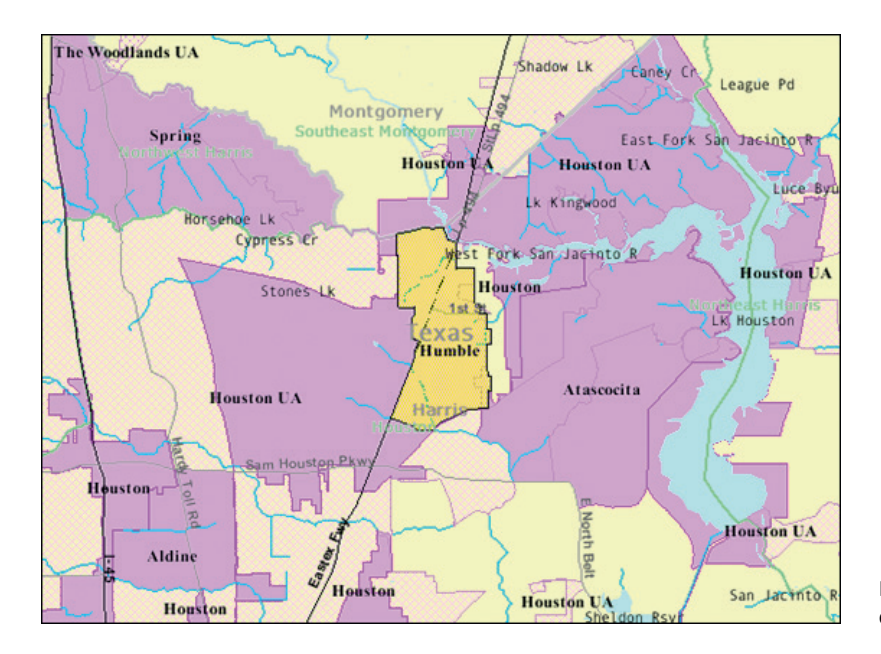


Fig. 9 - Geographical location of the Humble salt dome.

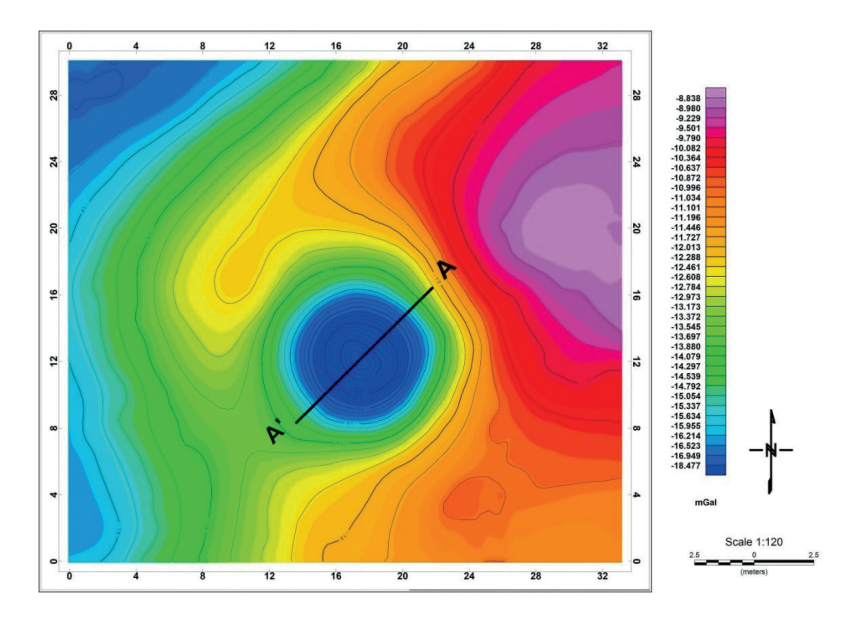


Fig. 10 - The Humble salt dome residual gravity field (the location of profile AA' is marked on the anomaly).

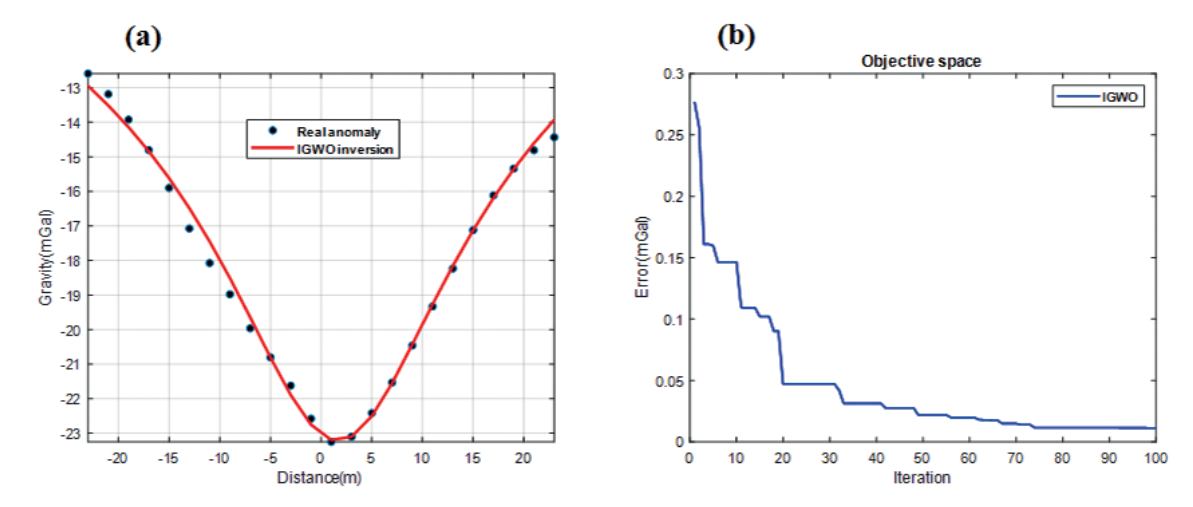


Fig. 11 - The effect of the gravity anomaly generated by profile AA' (black circles) and the effects calculated from the IGWO inversion (red curve) (a) and the convergence diagrams associated with the target function based on the number of iterations to obtain the best response using the IGWO for the Humble salt dome (b).

Table 6 - Estimated parameters of the Humble salt dome, U.S.A.

Model parameters	A (mGal×km²)	z (km)	q	<i>x</i> ₀ (km)
Search range	-500 - 0	0 - 30	0 - 2	-5 - 5
Abdelrahman et al. (2001a)	-258.1	4.96	1.42	
Salem <i>et al.</i> (2003)		5.15		
Tlas et al. (2005)	-283.14	4.59	1.47	0.01
Afshani and Tlas (2012)	-279.81	4.58	1.48	
Mehanee (2014)	-292.54	4.62	1.5	
Biswas (2015)	-275.6	4.4	1.5	0.07
Present method (IGWO)	-270.32	4.54	1.51	-0.05

5.2. The Aji Chay salt dome

The Aji Chay salt dome is situated in north-western Iran. This region contains sandstone, conglomerate and marl deposits as well as evaporite sediments that have undergone severe erosion due to loose facies. The salt domes in this region are often shallow and contain potash alloy. Fig. 13 shows the Bouguer gravity anomaly after gravity corrections. Fig. 14 illustrates the residual gravity anomaly after quadratic trendline elimination. Fig. 14 shows the BB' profile in the E-W direction at a length of 84 m. Data collection was carried out along the profile at 2-metre distances. Fig. 15 shows the anomaly generated by profile BB' and the inverse modelling results obtained using the IGWO. Table 7 provides the results obtained by implementing the method discussed above with the residual gravity anomaly where the depth to the centre of the model was 63.38 m and a geometric shape factor of 1.49 was obtained, which was consistent with the results of a report by the National Geological and Mineral Exploration Organisation (Razavi and Jafari, 2008) which seeked to estimate the depth, range, and shape of the Aji Chay salt dome (Table 7).

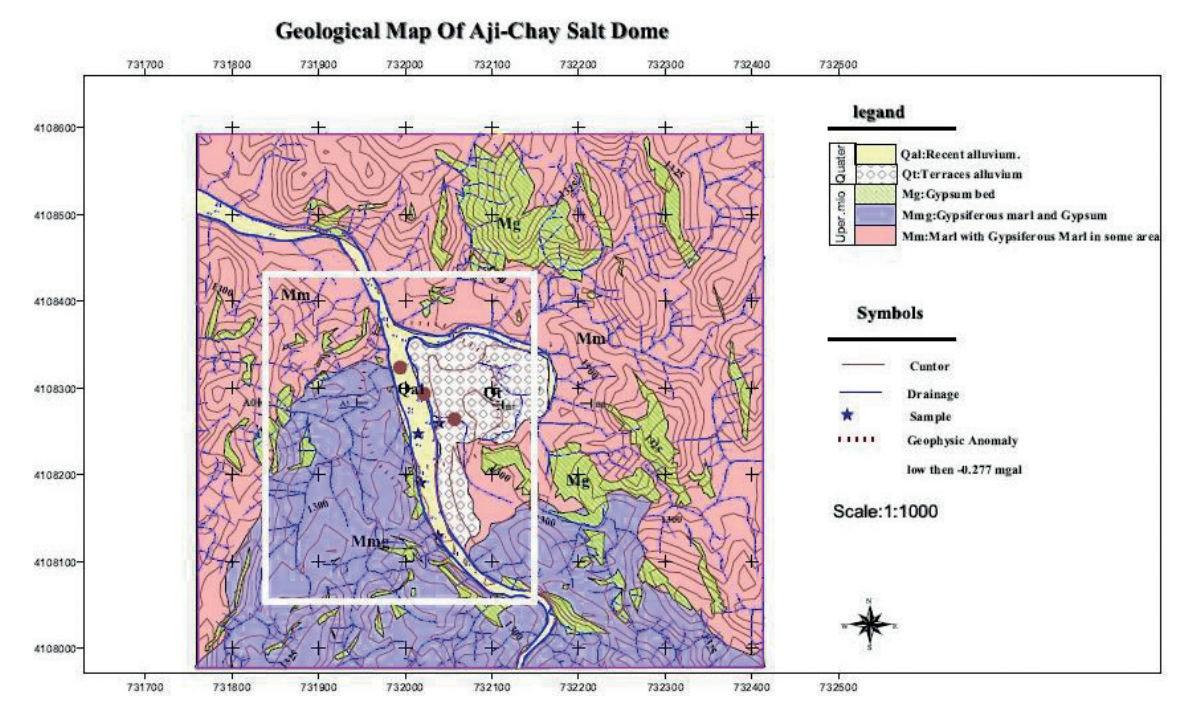


Fig. 12 - The Aji Chay geological map (the gravity datum collection area is marked with a white rectangle).

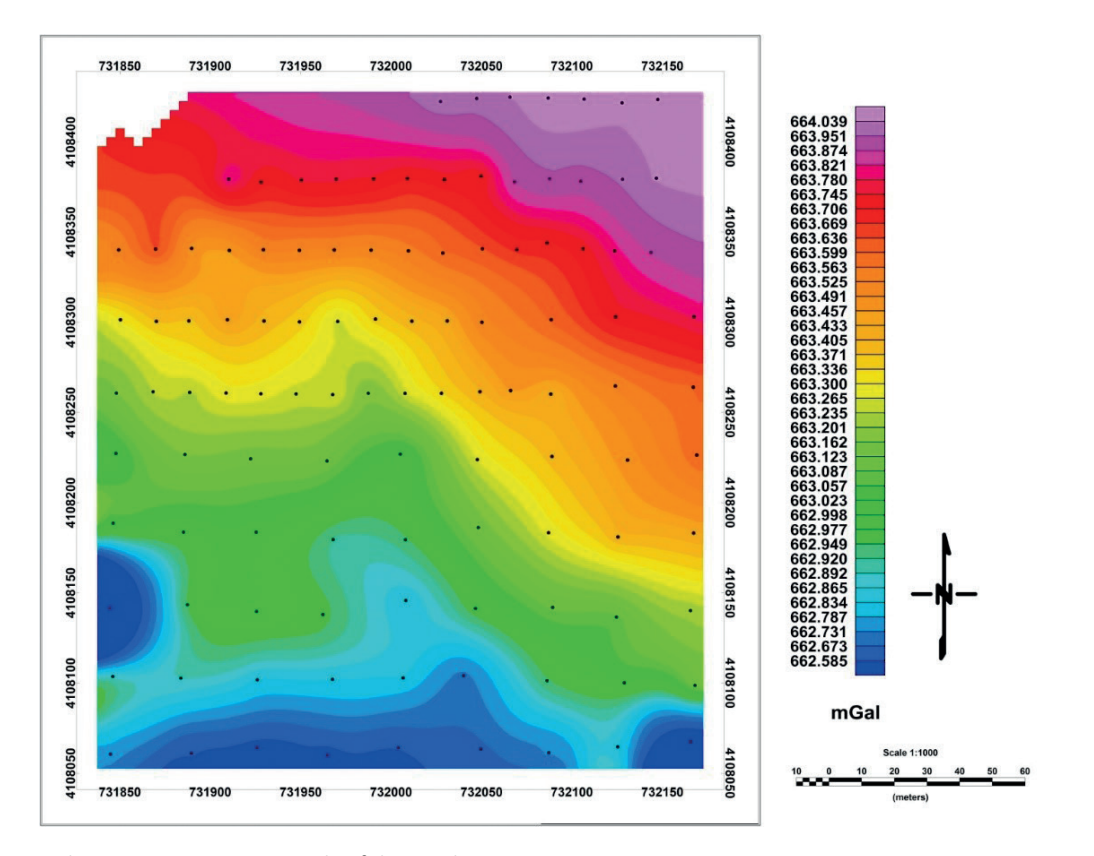


Fig. 13 - The Bouguer gravity anomaly of the Aji Chay region.

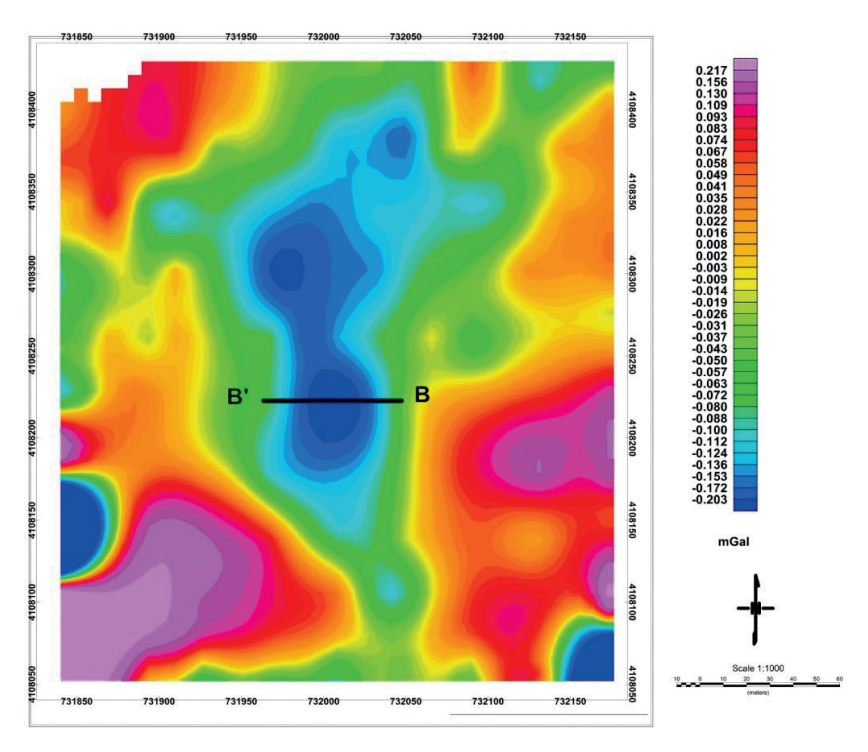


Fig. 14 - The Aji Chay salt dome residual gravity field (the location of profile BB' is marked on the anomaly).

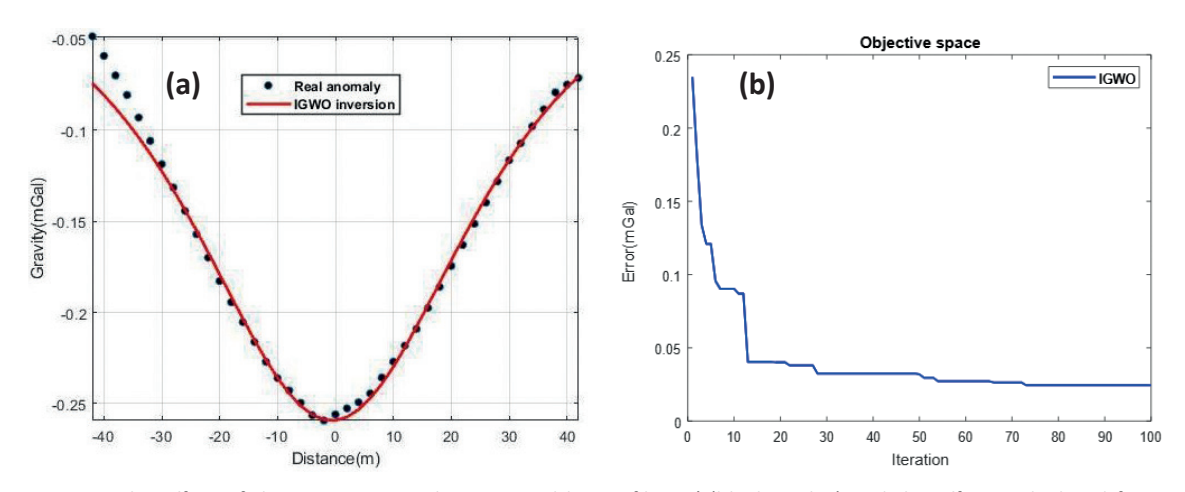


Fig. 15 - The effect of the gravity anomaly generated by profile BB' (black circles) and the effects calculated from the IGWO inversion (red curve) (a) and the convergence diagrams associated with the target function based on the number of iterations to obtain the best response using the IGWO for the Aji Chay salt dome (b).

Table 7 - Estimated parameters of the Aji Chay salt dome, Iran.

Model parameters	A (mGal×km²)	z (km)	q	<i>x</i> ₀ (km)
Search range	-500 - 0	0 - 60	0 - 2	-5 - 5
Present method (IGWO)	-331.62	63.38	1.49	-0.12
Pourreza and Hajizadeh (2019)		65	1.5	

6. Discussion and conclusions

The present study used the GWO algorithm, a nature-based swarm algorithm, to interpret the residual gravity data generated by simple geometrical shapes with and without noise and employed real gravity anomaly to estimate the parameters of amplitude coefficient, depth, shape factor, and the centre position of gravity anomalies. The synthetic models of the sphere and horizontal and vertical cylinder were investigated, and the IGWO managed to estimate the unknown parameters of the model with good accuracy (Tables 1 to 3). As demonstrated, the RMSE assessed between the initial and the estimated gravity anomaly parameters was 0.00003 mGal, 0.0099 mGal, and 0.616 mGal without noise, and 0.0499 mGal, 1.034 mGal, and 6.994 mGal with a 10% noise for the sphere, horizontal-cylinder, and vertical-cylinder models, respectively, all of which are insignificant amounts indicating the excellent responses yielded by the IGWO.

The other synthetic model investigated in the present study was a composite model encompassing a vertical cylinder at a low depth as the target anomaly and the two sphere and horizontal-cylinder models as interfering anomalies, where the calculated parameters indicated acceptable error compared to the initially assumed values for the vertical-cylinder model and strong and acceptable results were obtained (Table 5). As observed, the algorithm became convergent after the 68th iteration, and the value of the target function reached 0.096 without noise and 0.145 with a 7% noise in the 38th iteration (Figs. 7 and 8).

The IGWO was also used to invert two real gravity profiles, where the estimated parameters were calculated to be close to the results of previous studies, thus, indicating the proper performance of the algorithm (Tables 6 and 7). As Figs. 11b and 15b show, the value of the target function reached 0.011 in the final iteration for the Humble salt dome and 0.023 for the Aji Chay salt dome.

In general, the advantages of using the IGWO algorithm as an intelligent optimisation tool in modelling are that this method:

- by limiting the search space, improves the issue of non-uniqueness in the results and converges quickly without getting stuck in a local minimum;
- returns the initial assumed values to the real value of the parameter, which is very favourable in geophysical explorations;
- estimates all unknown parameters simultaneously with good accuracy and does not need to calculate the derivative;
- presents a processing time that is extremely low and has few parameters to adjust in comparison to other algorithms.

Finally, according to the mentioned advantages, it is recommended to use this method in solving various problems related to the interpretation of geophysical data. These include real data as well as exploration projects where there are several sources with distance.

REFERENCES

Abdelrahman E.-S.M. and El-Araby H.M.; 1993: *Shape and depth solutions from gravity data using correlation factors between successive least-squares residuals*. Geophys., 59, 1785-1791, doi: 10.1190/1.1443393.

Abdelrahman E.-S.M. and Sharafeldin S.M.; 1995a: *A least-squares minimization approach to shape determination from gravity data.* Geophys., 60, 589-590.

Abdelrahman E.-S.M. and Sharafeldin S.M.; 1995b: A least-squares minimization approach to depth determination from numerical horizontal gravity gradients. Geophys., 60, 1259-1260.

Abdelrahman E.-S.M., Bayoumi A.I., Abdelhady Y.E., Gobashy M.M. and El-Araby H.M.; 1989: *Gravity interpretation using correlation factors between successive least-squares residual anomalies.* Geophys., 54, 1614-1621, doi: 10.1190/1.1442629.

- Abdelrahman E.-S.M., Bayoumi A.I. and El-Araby H.M.; 1991: A least-squares minimization approach to invert gravity data. Geophys., 56, 115-118.
- Abdelrahman E.-S.M., El-Araby T.M., El-Araby H.M. and Abo-Ezz E.R.; 2001: *A new method for shape and depth determinations from gravity data*. Geophys., 66, 1774-1780.
- Agarwal A., Chandra A., Srivastava S. and Singh R.K.; 2018: *Grey wolf optimizer: a new strategy to invert geophysical data sets.* Geophys. Prospect., 66, 1215-1226, doi: 10.1111/1365-2478.12583.
- Al-Attar M., El-Gaafary A.A.M., Yahia S.M. and Hemeida A.M.; 2015: Design static VAR compensator controller using artificial neural network optimized by modify Grey Wolf Optimization. In: Proc. International Joint Conference on Neural Networks (IJCNN) 2015, Killarney, Ireland, doi: 10.1109/IJCNN.2015.7280704.
- Asfahani J. and Tlas M.; 2008: *An automatic method of direct interpretation of residual gravity anomaly profiles due to spheres and cylinders.* Pure Appl. Geophys., 165, 981-994.
- Asfahani J. and Tlas M.; 2012: Fair function minimization for direct interpretation of residual gravity anomaly profiles due to spheres and cylinders. Pure Appl. Geophys., 169, 157-165, doi: 10.1007/s00024-011-0319-x.
- Babu L.A., Reddy K.G. and Mohan N.L.; 1991: *Gravity interpretation of vertical line element and slap a Mellin transform method.* Indian J. Pure Appl. Math., 22, 439-447.
- Barbosa V.C.F. and Silva J.B.C.; 1994: Generalized compact gravity inversion. Geophys., 59, 57-68, doi: 10.1190/1.1443534.
- Biswas A.; 2015: Interpretation of residual gravity anomaly caused by simple shaped bodies using very fast simulated annealing global optimization. Geosci. Front., 6, 875-893.
- Bosch M.; 1999: Lithologic tomography: from plural geophysical data to lithology estimation. J. Geophys. Res., Solid Earth, 104, 749-766.
- Boulanger O. and Chouteau M.; 2001: Constraints in 3D gravity inversion. Geophys. Prospect., 49, 265-280.
- Calcagno P., Chiles J.P., Courrioux G. and Guillen A.; 2008: *Geological modelling from data and geological knowledge: part I. Modelling method coupling 3D potential-interpolation and geological rules.* Phys. Earth Planet. Inter., 171, 147-157.
- Chahar V. and Kumar D.; 2017: An astrophysics-inspired Grey wolf algorithm for numerical optimization and its application to engineering design problems. Adv. Eng. Software, 112, 231-254.
- Eshaghzadeh A. and Hajian A.; 2020: Multivariable Modified Teaching Learning Based Optimization (MM-TLBO) algorithm for inverse modeling of residual gravity anomaly generated by simple geometric shapes. J. Environ. Eng. Geophys., 25, 463-476.
- Eshaghzadeh A. and Sahebari S.S.; 2020: Multivariable Teaching Learning Based Optimization (MTLBO) algorithm for estimating the structural parameters of the buried mass by magnetic data. Geofizika, 37, 213-235, doi: 10.15233/gfz.2020.37.6.
- Essa K.S.; 2007: A simple formula for shape and depth determination from residual gravity anomalies. Acta Geophysica, 55, 182–190, doi: 10.2478/s11600-006-0048-3.
- Essa K.S.; 2014: New fast least-squares algorithm for estimating the best-fitting parameters due to simple geometric-structures from gravity anomalies. J. Adv. Res., 5, 57-65, doi: 10.1016/j.jare.2012.11.006.
- Essa K.S. and Elhussein M.; 2018: *PSO (Particle Swarm Optimization) for interpretation of magnetic anomalies caused by simple geometrical structures.* Pure Appl. Geophys., 175, 3539-3553.
- Fedi M.; 2007: DEXP: a fast method to determine the depth and the structural index of potential fields sources. Geophys., 72, I1-I11.
- Gupta O.P.; 1983: A least-squares approach to depth determination from gravity data. Geophys., 48, 357-360.
- Hartman R.R., Teskey D. and Friedberg I.; 1971: A system for rapid digital aeromagnetic interpretation. Geophysics, 36, 891–918, doi: 10.1190/1.1440213.
- Heidari A.A. and Pahlavani P.; 2017: An efficient modified grey wolf optimizer with Lévy flight for optimization tasks. Appl. Soft Comput., 60, 115-134, doi: 10.1016/j.jare.2012.11.006.

- Jadhav A.N. and Gomathi N.; 2017: WGC: hybridization of exponential grey wolf optimizer with whale optimization for data clustering. Alexandria Eng. J., 57, doi: 10.1016/j.aej.2017.04.013.
- Kamboj V.K.; 2016: A novel hybrid PSO-GWO approach for unit commitment problem. Neural Comput. Appl., 27, 1643-1655.
- Kilty T.K.; 1983: Werner deconvolution of profile potential field data. Geophysics, 48, 234–237, doi: 10.1190/1.1441465.
- Li S.Y., Wang S.M., Wang P.F., Su X.L., Zhang X.S. and Dong Z.H.; 2018: *An improved grey wolf optimizer algorithm for the inversion of geoelectrical data*. Acta Geophys., 66, 607-621, doi: 10.1007/s11600-018-0148-8.
- Li X. and Chouteau M.; 1998: Three-dimensional gravity modeling in all space. Surv. Geophys., 19, 339-368.
- Li Y. and Oldenburg D.W.; 1998: 3-D inversion of gravity data. Geophys., 63, 109-119.
- Mehanee S.A.; 2014: Accurate and efficient regularised inversion approach for the interpretation of isolated gravity anomalies. Pure Appl. Geophys., 171, 1897-1937, doi: 10.1007/s00024-013-0761-z.
- Mirjalili S., Mirjalili S.M. and Lewis A.; 2014: Grey wolf optimizer. Adv. Eng. Software, 69, 46-61.
- Mittal N., Singh U. and Sohi B.S.; 2016: *Modified grey wolf optimizer for global engineering optimization*. Appl. Comput. Intell. Soft Comput., 2016, doi: 10.1155/2016/7950348.
- Mohan N.L., Anandababu L. and Roa S.; 1986: *Gravity interpretation using Mellin transform.* Geophys., 52, 114-122.
- Muangkote N., Sunat K. and Chiewchanwattana S.; 2014: *An improved grey wolf optimizer for training q-Gaussian radial basis functional-link nets.* In: International Computer Science and Engineering Conference (ICSEC) 2014, Khon Kaen, Thailand, pp. 209-214, doi: 10.1109/icsec.2014.6978196.
- Nandi B.K., Shaw R.K. and Agarwal N.P.; 1997: A short note on identification of the shape of simple causative sources from gravity data. Geophys. Prospect., 45, 513-520.
- Odegard M.E. and Berg J.W.; 1965: *Gravity interpretation using the Fourier integral*. Geophysics, 30, 424–438, doi: 10.1190/1.1439563.
- Pourreza S. and Hajizadeh F.; 2019: Simulation of a salt dome using 2D linear and nonlinear inverse modelling of residual gravity field data. Bulletin of the Mineral Research and Exploration, 160, 231–244, doi: 10.19111/bulletinofmre.502021.
- Reid A.B., Allsop J.M., Granser H., Millett A.J. and Somerton I.W.; 1990: *Magnetic interpretation in three dimensions using Euler deconvolution*. Geophysics, 55, 80-91, doi: 10.1190/1.1442774.
- Roshan R. and Singh U.K.; 2017: *Inversion of residual gravity anomalies using tuned PSO*. Geosci. Instrum. Methods Data Syst., 6, 71-79, doi: 10.5194/gi-6-71-2017.
- Rossi L., Reguzzoni M., Sampietro D. and Sansò F.; 2015: Integrating geological prior information into the inverse gravimetric problem: the Bayesian approach. In: Sneeuw N., Novak P., Crespi M. and Sansò F. (eds), VIII Hotine-Marussi Symposium of Mathematical Geodesy, Springer, Berlin, Germany, pp. 317-324, doi: 10.1007/1345_2015_57.
- Salem A., Elawadi E. and Ushijima K.; 2003: Short note: depth determination from residual anomaly using a simple formula. Comput. Geosci., 29, 801-804, doi: 10.1016/S0098-3004(03)00106-7.
- Santos F.A.M.; 2010: *Inversion of self-potential of idealized bodies' anomalies using particle swarm optimization*. Comput. Geosci., 36, 1185-1190.
- Sharma B. and Geldart L.P.; 1968: Analysis of gravity anomalies of two-dimensional faults using Fourier transforms. Geophys. Prospect., 16, 77-93.
- Shaw R.K. and Agarwal P.; 1990: The application of Walsh transforms to interpret gravity anomalies due to some simple geometrical shaped causative sources: a feasibility study. Geophys., 55, 843-850.
- Snieder R.; 1998: *The role of nonlinearity in inverse problems*. Inverse Prob., 14, 387-404, doi: 10.1088/0266-5611/14/3/003.
- Song X., Tang L., Zhao S., Zhang X., Li L. and Huang J.; 2015: *Grey wolf optimizer for parameter estimation in surface waves*. Soil Dyn. Earthquake Eng., 75, 147-157.

- Sulaiman M.H., Mustaffa Z., Daniyal H., Rusllim M.M. and Aliman O.; 2015: Solving optimal reactive power planning problem utilising nature inspired computing techniques. ARPN Journal of Engineering and Applied Sciences, 10, 10123–10130.
- Tarantola A.; 2005: *Inverse problem theory and methods for model parameter estimation*. SIAM, Elsevier Science Ltd, Amsterdam, The Netherlands, 630 pp.
- Thompson D.T.; 1982: *EULDPH a new technique for making computer-assisted depth estimates from magnetic data*. Geophysics, 47, 31–37.
- Tlas M., Asfahani J. and Karmeh H.; 2005: A versatile nonlinear inversion to interpret gravity anomaly caused by a simple geometrical structure. Pure and Applied Geophysics, 162, 2557–2571.
- Vashisth D., Routa A., Mohanty P. and Srivastava S.; 2019: Whale Optimization Algorithm a robust strategy to invert geophysical data sets. Presented at AGU Fall Meeting 2019.
- Yuan S., Shangxu W. and Nan T.; 2009: Swarm intelligence optimization and its application in geophysical data inversion. Appl. Geophys., 6, 166-174.
- Zhu A., Xu C., Li Z., Wu I. and Liu Z.; 2015: *Hybridizing grey wolf optimization with differential evolution for global optimization and test scheduling for 3D stacked SoC.* J. Syst. Eng. Electron., 26, 317-328, doi: 10.1109/JSEE.2015.00037.

Corresponding author: Afshin Akbari Dehkharghani

Department of Petroleum, Mining and Materials Engineering, CT.C., Islamic Azad University

Ashrafi Isfahani st., Imam Hasan blv., Tehran, Iran

Phone: +98 9121202754; e-mails: a.akbari dekhovarghani@iautcb.ac.ir, afshinkr@gmail.com